Stress monitoring of plates by means of nonlinear guided waves

Meng Wang and Annamaria Pau[1][0000−0002−4946−0302]

Sapienza University of Rome, Department of Structural and Geotechnical Engineering
via Eudossiana 18, 00184 Rome, Italy
wang.1856445@studenti.uniroma1.it
annamaria.pau@uniroma1.it

Abstract. We investigate the propagation of nonlinear guided waves in plates in view of their application to the identification of the state of stress. The study is performed modelling via Finite Elements the propagation of Lamb waves in a prestressed plate, whose equations of motion are a second-order approximation accounting for both geometric and material nonlinearities. Different intial prestress conditions are investigated, parallel and orthogonal to the direction of wave propagation. A couple of physical phenomena presenting remarkable sensitivity to initial stress emerged using the resonant couple of S1-S2 modes. First, the increase of the secondary wave amplitude with propagation distance is clearly observed together with the sensitivity of the second-harmonic amplitude to the initial state of prestress. Second, a subharmonic and superharmonics are observed, due to the interaction between primary and secondary waves.

Keywords: Guided waves · nonlinear ultrasounds · secondary harmonic · stress monitoring.

1 Introduction

Nonlinear ultrasonic guided waves combine the advantages of nonlinear ultrasound and ultrasonic guided waves. The resulting increase in sensitivity to stress, defects, fatigue, etc., makes them advantageous over the linear ultrasonic guided waves in tests on prestressed materials [1].

Since the 1960s, many researchers have investigated higher harmonic generation from guided ultrasonic waves in view of their applications to nondestructive evaluation (NDE)[2] and structural health monitoring (SHM). Many studies concerning the second harmonic generation of ultrasonic guided waves are by Deng [3, 4], with particular regard to the analytical and numerical investigation of the cumulative second harmonics of shear-horizontal (SH) and Rayleigh-Lamb (RL) waves in plates. Following these findings, De Lima and Hamilton [5] developed the analytical framework necessary to explain the internal resonance beteween

primary and secondary modes, which requires synchronism (i.e. equality of phase velocities and group velocities) and nonzero power flux. There are in the literature some contradictory results concerning the generation of higher harmonics, once given the symmetry of the primary wave. A contribution to untangle the matter was provided by Müller et al. [7]. In this line of research are the contributions by Srivastava and Lanza di Scalea [6], showing the inability of a symmetric primary harmonic wave to generate antisymmetric second harmonics, as well as that from Chillara and Lissenden [8] who investigated the interaction of multiple primary modes and the generation of third harmonics. This paper considers only RL modes. The primary mode which generates a strong second harmonic is chosen based on the above mentioned advances.

The propagation speed of elastic waves in a prestressed solid not only depends on the second-order elastic constants and density of the material, but is also related to higher-order elastic constants and initial stress. The relationship between velocity and stress can be obtained by means of the theory called acoustoelasticity [9], which employs a model accounting for geometric and material nonlinearities in its linearized form [10]. Higher order approximations of the same model can be treated by the perturbative approach [11], providing information on the occurence of higher harmonics. Many authors [5–8, 11] treat these nonlinearities as a second-order perturbation of the linear response, and express the associated secondary wave field as a linear superposition of the normal wave modes obtained from the linear free-vibration problem. The secondary wave field results from the forced response of a linearized equation, whose solution can be obtained using the approach presented by Auld [12] for linear waveguides subjected to body and surface forces.

This work presents an investigation of the RL wave propagation in a prestressed plate via the finite element method, accounting for the effects of geometric and material nonlinearity. This model is investigated by using its second-order approximation [11], demonstrating the occurrence of a secondary harmonic, whose frequency is twice that of the primary wave, and elucidating the effects of the initial state of stress and propagation distance on the amplitude of the secondary wave. It is also shown that, due to the interaction between primary and secondary waves, a subharmonic emerges (whose frequency is the difference between secondary and twice the primary wave frequencies) as well as superharmonics (whose frequencies are the sum of the primary and secondary frequencies, plus further multiple interactions). Three different prestress states are studied, including: prestress in the direction of the wave propagation, prestress orthogonal to the direction of wave propagation, and plane isotropic stress in the plane of the plate.

2 Equations of motion

Three different configurations of the material points $\mathbf{P}$ are defined: natural configuration, free of stress and strains, initial configuration, which is a stressed and

strained static equilibrium state, and current configuration. The coordinates of a point $\mathbf{P}$ in the natural, initial and current configuration are named respectively $\mathbf{a}(\mathbf{P})$, $\mathbf{X}(\mathbf{P})$, and $\mathbf{x}(\mathbf{P})$. Strains are defined using the Green–Lagrange strain tensor: $\mathbf{E}^f = \frac{1}{2}(\nabla\mathbf{x}\nabla\mathbf{x}^T - \mathbf{I})$, where the derivatives of ∇ are with respect to the natural coordinates $\mathbf{a}$.

The balance equations are set up in the current configuration, by using the first Piola–Kirchhoff stress tensor $\mathbf{S}$ and differentiating with respect to the natural coordinates:

$$\mathrm{Div}\mathbf{S} = \rho_0\ddot{\mathbf{u}} \tag{1}$$

where ρ_0 is the density in the natural state, the double dots stand for double time derivative. In addition, it is assumed $\ddot{\mathbf{x}} = \ddot{\mathbf{u}}$, where $\mathbf{u}$ is an infinitesimal displacement superimposed on the initial configuration, which is reached by superimposing to the natural configuration a static displacement $\boldsymbol{\alpha}\mathbf{a}$, with $\boldsymbol{\alpha}$ representing a homogeneous transformation.

The relation between the Cauchy stress tensor $\mathbf{T}$ and the first Piola-Kirchoff stress tensor $\mathbf{S}$ for a hyperelastic material is:

$$\mathbf{S} = \nabla\mathbf{x}\mathbf{T} \qquad \text{with} \quad T_{ij} = \frac{\partial\Phi}{\partial E^f_{ij}} \tag{2}$$

where Φ is the strain energy function, which, considering an isotropic material, can be expressed as:

$$\Phi = (\frac{\lambda+2\mu}{2})I_1^2 + 2\mu I_2 + (\frac{l+2m}{3})I_1^3 + 2mI_1I_2 + nI_3 \tag{3}$$

where $I_1 = tr\mathbf{E}^f$, $I_2 = (tr\mathbf{E}^f)^2 - tr(\mathbf{E}^{f^2})$, and $I^3 = det\mathbf{E}^f$, λ and μ are the Lamé constants and l, m and n are the Murnaghan third-order elastic constants.

Based on this model, the Navier equations of motion are obtained, then their second-order approximation is retrieved according to the following rule: in terms not involving components of $\nabla\mathbf{u}$, the first, second and third power of $\boldsymbol{\alpha}$ will be retained; in the coefficients of $\nabla\mathbf{u}$ components, the first and second power of $\boldsymbol{\alpha}$ will be retained; no term involving $\nabla\mathbf{u}$ to a power higher than two will be retained.

3 Finite Element simulations

This section presents the results of a FE simulation based on the second-order approximation of the equations of motion obtained as described in the previous Section. The FE model was created in COMSOL Multiphysics with general form PDE modulus. Fig. 1 shows the sketch of the domain where the equations of motion are enforced, that consists of 2D area 10mm thick and 2000mm long,

representing a plate with upper and lower surfaces free of stress, made of 7075-T651 Aluminum (Table 1). A state of plane strain is assumed for the propagating waves, which corresponds to a displacement field with two components u_1 and u_3, with $u_2 = 0$ (see Figure 1a). In plates, bulk waves experience repeated reflections on the upper and lower surfaces alternatively. The disturbance resulting from this mutual interference is guided by the plate surfaces and is directed along the plane of the plate.

RL waves can be excited by applying a disturbance at some boundary. In our case, a sinusoidal pulse modulated in time by a Gaussian function as in Fig. 1 (b) is applied as Dirichlet boundary condition on the left end of the plate (Fig. 1 (a)). This side-incidence method can be used to generate symmetric as well as asymmetric modes, in accordance with the distribution of the disturbance along the plate thickness. Moreover, a fixed boundary condition was assigned to the right end of the plate, which does not affect the calculations within a given time frame.

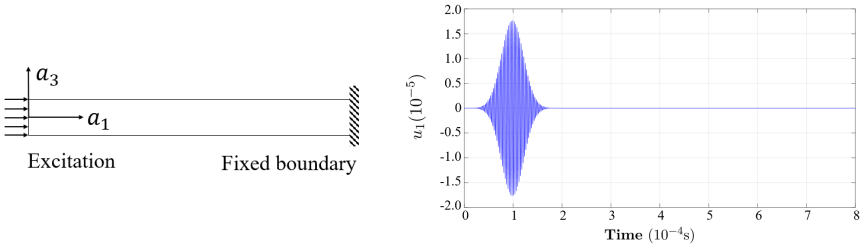

(a) Sketch of the 2D FE plate model in COMSOL

(b) Excitation signal

Fig. 1. FE settings in COMSOL.

In the FE analysis, to ensure the accuracy of the simulations, the discretization was refined so as to include at least 10 elements per wavelength, which, in this case, has to be scaled according to the shorter wavelength of the second harmonic. The same applies to time discretization in relation to wave frequency. The elements used in this study have quadratic shape functions.

Table 1. Material properties of 7075-T651 Aluminum.

ρ_0 (kg/m^3)	λ (GPa)	μ (GPa)	l (GPa)	m (GPa)	n (GPa)
2810	52.3	26.9	-252.2	-325	-351.2

Three different states of prestress are investigated, specifically: uniaxial stress in the direction of the wave propagation (a_1, case A), uniaxial stress orthogonal to the direction of wave propagation (a_2, case B), and a plane state of stress in the plane (a_1, a_2) with equal principal stresses along the two directions a_1, a_3 which is called plane-isotropic state (case C). The corresponding strains are reported in Table 2 (ν=0.34). For each of the A, B, and C cases, both $\alpha > 0$ (tensile strain) and $\alpha < 0$ (compression strain) are investigated. It is taken $\alpha = 0.004$, which is about 50% of the yielding strain for 7075-T651 Aluminum.

Table 2. States of prestrain

	α_1	α_2	α_3
case A	α	$-\nu\alpha$	$-\nu\alpha$
case B	$-\nu\alpha$	α	$-\nu\alpha$
case C	α	α	$-\nu\alpha$

4 The second-harmonic resonant wave

The analysis of nonlinear harmonic generation was limited to the second-order nonlinearity. The second-harmonic generation should satisfy the following internal resonance requirements: equality of phase and group velocities between the primary mode and the higher-harmonic mode, and nonzero power flux. Figure 2 shows the dispersion diagrams in terms of group and phase velocity for an unstressed Aluminum plate. It can be seen that, on exciting mode S1 at a frequency of 355kHz with a plate 10mm in thickness (3.55MHz*mm), there is a resonant higher harmonic S2 mode at 710kHz. It is known that between these two modes there is a nonzero power flux [5, 11].

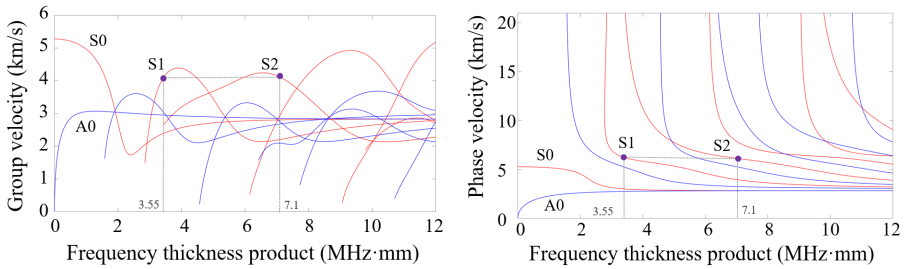

(a) Group velocity (b) Phase velocity

Fig. 2. Group and phase velocity matching of 7075-T651 Aluminum in the absence of prestress and the couple of resonance primary and secondary waves.

Figure 3(a) reports the contour plot of the displacement u_1 at a given time instant, where on the right the S1 mode can be recognized, while on the left the superposition between S1 and S2 modes appears. Figure 3(b) shows the Fourier transform of the time-history of the response in terms of u_1, 50mm away from the left end of the plate on the upper surface. The primary wave is the S1 mode, and the second harmonic S2 generated by the internal resonance is apparent from the second smaller peak.

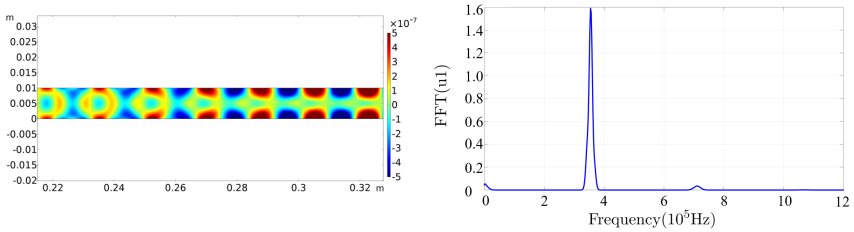

(a) (b)

Fig. 3. (a) u_1 displacement contour plot at $t = 1.7 \times 10^{-4}s$ (b) Fourier Transform of the time-history of the response in terms of u_1 on the upper surface.

4.1 Dependence of the response on the initial state of prestress

To quantify the degree of nonlinearity in the response, a relative nonlinear parameter β' was introduced in [13], which is defined as:

$$\beta' = \frac{A_2}{A_1^2} \tag{4}$$

where A_1 and A_2 are the frequency-domain amplitudes of the primary (at the excitation frequency) and of the secondary (twice the excitation frequency) waves.

Figure 4 reports the amplitude of the Fourier transforms of the time-history of the component u_1 on the plate surface for discrete points at increasing distances for a case of unstressed initial conditions. The maximum amplitude, pertaining to the secondary wave, is centered at the measurement point. It is apparent that the amplitude of the second-harmonic increases with the propagation distance, as expected from analytical results [5]. The magnitudes of the nonlinear parameter, as a function of the propagation distance in different prestressed conditions, are shown in Figure 5(a). This figure shows that there is a linear increase in the relative nonlinear parameter β' with increasing propagation distance. The slope associated to case C is the largest, while case B has the lowest slope, even smaller than the free-stress case.

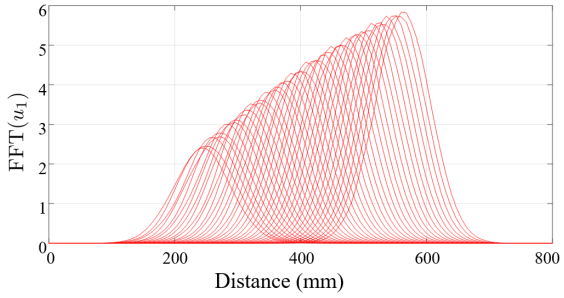

Fig. 4. Amplitude of the Fourier transform of the t-h response for discrete points at increasing distance in free-stress initial condition.

The parameter β' also changes as a function of the amount of initial prestrain. Figure 5(b) reports the relative nonlinear parameter for the different prestress states as a function of α. A linear increase in the relative nonlinear parameter β' with increasing α is observed in cases A and C, which corresponds to a cumulative second harmonic generation for the selected S1–S2 mode pair. Also, in case B, the magnitude of β' linearly increases for increasing α, but it is out-of-phase with respect to the primary wave.

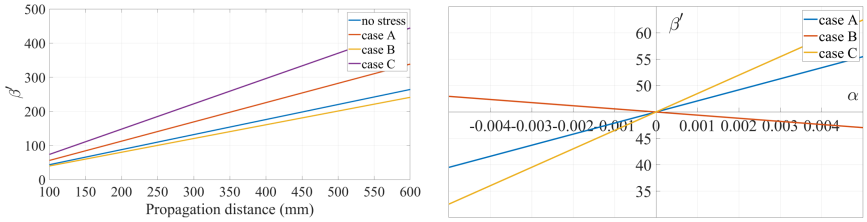

Fig. 5. (a) β' as a function of the propagation distance of the pair S1–S2, considering α=0.004 in cases A, B, and C. (b) β' as a function of the initial prestrain α for the pair S1–S2, 100mm away from the left boundary.

4.2 Resonance condition and interaction between primary and secondary waves

The FE analysis enabled the observation of how the resonance sets in and how primary S1 and secondary S2 wave modes interact. Figure 6 reports the normalized spectrum (FFT of the response divided by its maximum) of the component u_1 of the displacement field on the plate surface at different distances measured from the left free end, for an S1 mode with the central frequency of the disturbance in resonance conditions (355 kHz (a)) and off-resonance (400 kHz (b)), in an unstressed plate. It is obvious that when the central frequency is in resonance, the amplitude of the second-harmonic can theoretically increase indefinitely in space (Figure 6 a), as it is known from the multiple-scale solution of the equations of motion [5, 11]. When the central frequency is off-resonance, instead, there is still a second-harmonic, however, its amplitude does not increase as the waves travels along the plate. When the plate is prestressed, the resonant frequency slightly changes. Hence, it can be inferred that, once known the resonance condition in the unstressed plate, a change in the stress state is detectable by the change of the resonant frequency.

Figures 6 a and b also show that the primary and the secondary waves interact with each other. Interaction is unavoidable due to the fact that the frequency content of the disturbance has a frequency band which, though narrow, excites also neighboring frequencies, besides the central frequency of the disturbance. Therefore, there is a certain amount of detuning which causes the occurrence

of a near-zero frequency subharmonic (difference between twice the frequency of the primary and the secondary wave), the second-harmonic, plus several superharmonics at frequencies which are linear combinations of the primary and secondary frequencies [14]. In this regard, it is apparent from Figure 6a that, in resonance conditions, the third harmonic is highly sensitive to the nonlinearity. This makes the third harmonic a good candidate to be observed in nondestructing evaluation procedures.

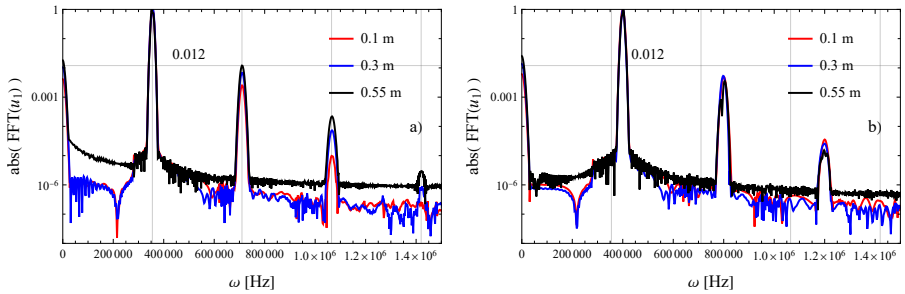

Fig. 6. Normalized spectrum of the displacement u_1 of points at different distances from the left free end on the plate surface for different central frequencies of the disturbance (a) 355 kHz (b) 400 kHz

5 Conclusion

In this work, we studied the nonlinear guided wave propagation in prestressed Aluminum plates associated with the second harmonic generation by using 2D FE simulations. The model employed is a second-order approximation accounting for material and geometric nonlinearities. Three different states of prestress are considered, that are: uniaxial stress in the direction of the wave propagation (case A), uniaxial stress orthogonal to the direction of wave propagation (B), and plane state of stress in the plane of the plate (C).

The relative nonlinear parameter β' was introduced to quantity the degree of nonlinearity in the response. The nonlinear parameter dependence with different initial states of prestress is investigated, and it is shown that it presents a linear increase with the increasing of tensile stress in cases A and C, and a linear increase in magnitude but opposite phase in case B. Case C is tied to the largest variation. Besides, in resonance conditions, the nonlinear parameter linearly increases with the propagation distance, while, when we are off-resonace, the contribution of the second harmonic does not vary in space. This characteristic of the response can be used to indicate a change in the state of stress, which, in turn, implies a change of the resonant frequency. Finally, a subharmonic and superharmonics were also observed.

References

1. Zhao, C., Tanweer, S., Li, J., Lin, M., Zhang, X., Liu, Y.: Nonlinear guided wave tomography for detection and evaluation of early-life material degradation in plates. Sensors **21**(16), 5498 (2021)
2. Liu, Y., Chillara, V.K., Lissenden, C.J.: On selection of primary modes for generation of strong internally resonant second harmonics in plate. Journal of Sound and Vibration **332**(19), 4517–4528 (2013)
3. Deng, M.: Cumulative second-harmonic generation accompanying nonlinear shear horizontal mode propagation in a solid plate. Journal of Applied Physics **84**(7), 3500–3505 (1998)
4. Deng, M.: Cumulative second-harmonic generation of Lamb-mode propagation in a solid plate. Journal of Applied Physics **85**(6), 3051–3058 (1999)
5. De Lima, W.J.N., Hamilton, M.F.: Finite-amplitude waves in isotropic elastic plates. Journal of sound and vibration **265**(4), 819–839 (2003)
6. Srivastava, A., Di Scalea, F.L.: On the existence of antisymmetric or symmetric Lamb waves at nonlinear higher harmonics. Journal of Sound and Vibration **323**(3–5), 932–943 (2009)
7. Müller, M.F., Kim, J.Y., Qu, J., Jacobs, L.J.: Characteristics of second harmonic generation of Lamb waves in nonlinear elastic plates. The Journal of the Acoustical Society of America **127**(4), 2141–2152 (2010)
8. Chillara, V.K., Lissenden, C.J.: Interaction of guided wave modes in isotropic weakly nonlinear elastic plates: Higher harmonic generation. Journal of Applied Physics **111**(12), 124909 (2012)
9. Murnaghan, F.D.: Finite Deformation of an Elastic Solid. New Ed edition. Dover Publications (1967)
10. Pau, A., Vestroni, F.: The role of material and geometric nonlinearities in acoustoelasticity. Wave Motion, **86**, 79-90 (2019)
11. Pau, A., Lanza Di Scalea, F.: Nonlinear guided wave propagation in prestressed plates. Journal of Acoustical Society of America, **137**(3), 1529-1540 (2015)
12. Auld, B.A.: Acoustic fields and waves in solids. 2nd edition. Krieger Publishing Company (1990)
13. Wan, X., Tse, P.W., Xu, G., Tao, T., Zhang, Q.: Analytical and numerical studies of approximate phase velocity matching based nonlinear S0 mode Lamb waves for the detection of evenly distributed microstructural changes. Smart Materials and Structures, **25**, 045023 (2016)
14. Nayfeh, A.H., Mook, D.T.: Nonlinear Oscillations. John Wiley and Sons Ltd (1995)